UNIVERSITY OF WEST BOHEMIA

Applied and Computational Mechanics 4 (2010) 15–24

Applied and Computational Mechanics

Shape optimization of supersonic ejector for supersonic wind tunnel

V. Dvořák[a,*]

[a] *Faculty of Mechanical Engineering, Technical University of Liberec, Studentská 2, 461 17 Liberec, Czech Republic*

Received 28 August 2009; received in revised form 14 July 2010

Abstract

The article deals with the shape optimization of a supersonic ejector for propulsion of an experimental supersonic wind tunnel. This ejector contains several primary nozzles arranged around the mixing chamber wall. CFD software Fluent was used to compute the flow in the ejector. A dynamic mesh method was applied to find an optimal shape of the three-dimensional geometry. During the work it was found out that the previously developed optimization method for subsonic ejectors must be modified. The improved method is more stable and the solution requires fewer optimization steps. The shapes of the mixing chamber, the diffuser, inlet parts and the optimal declination of the primary nozzles are obtained as the optimization results.

Keywords: supersonic ejector, shape optimization, primary nozzle, wind tunnel

1. Introduction

Ejectors are used for many purposes, but the process is basically the same in every case: a high-pressure fluid (the primary stream) transfers part of its energy to a low pressure fluid (the secondary stream) and the resulting mixture is discharged at a pressure that lies between the driving pressure and the suction pressure. By the time that Keenan at al [1] performed the first comprehensive study of mixing, two cases of mixing were distinguished: the constant pressure mixing and the constant area mixing. However, nobody has yet established a definite link between the performance of constant area and constant pressure ejectors [2]. Many studies deal with optimization of some separated parameters of ejector or with intensification of the mixing process, as they are in a review carried out by Porter and Squyers [3] and published in 1976. Also nowadays many researchers investigate influences of separated design parameters. For example, Aphornratana and Eames [4] performed experiments on ejector with a moveable primary nozzle. An optimization of a suction chamber was done by Yadav and Patwardhan in work [5]. They designed the diameter of the suction chamber, the position of the primary nozzle and the angle of the necking of the suction chamber, but no optimization method was used. Grazzini and Rocchetti [6] used the numerical optimization to design a two-stage steam ejector for a cooling system. Only operational parameters were optimized, while the ejector construction was unchanged. Watanawanavet optimized a supersonic ejector in his thesis [7]. Again, separated parameters were optimized, no optimization method was used and the optimization missed complexity. Cizungu et al. [8] used a one-dimensional model of compressible flow to optimize an ejector for a cooling system. The results of this work were a determination of a suitable area ratio, the length of the mixing chamber and of the diffuser and several operation parameters.

*Corresponding author. Tel.: +420 485 353 479, e-mail: vaclav.dvorak@tul.cz.

Nowadays commercial CFD software is used by a large number of researchers. One of the first works using commercial CFD software to compute the flow in an ejector was work of Riffat et al. [9], who took into account incompressible fluid and turbulence model k-ε. Also software Fluent is widely used to compute flow both in supersonic and subsonic ejectors. E.g. Rusly et al. [10] used Fluent and segregated solver to compute flow in a supersonic ejector.

This study deals with aerodynamic optimization using dynamic mesh method provided by Fluent software. Ejector is optimized in a complex way. The shape of the ejector is given by normal cubic spline function, which allows obtaining an arbitrary shape, as it was presented by Dvořák in work [11]. Thus the resulting shape of the ejector is not limited by a choice of initial optimization parameters. A series of optimized shapes of the ejector for different values of relative back pressure was the result of these calculations. The resulting efficiencies were better than in a case of a simple ejector with constant area mixing chamber and with conic diffuser, as it was shown by Dvořák in work [12].

This work deals with shape optimization of a supersonic ejector for propulsion of an experimental supersonic wind tunnel with discontinuous operation. The scheme of the working principle and the arrangement of this kind of wind tunnel are obvious from fig. 1 adapted from the work [13] by Dvořák. The test section is placed in the suction tract of the ejector. The air flowing through the test section is sucked directly from the atmosphere. The flow properties like the turbulence intensity can be adjusted at the wind tunnel inlet. Compressed air supplied from pressure tanks is the primary medium for the propulsion of the wind tunnel in this case.

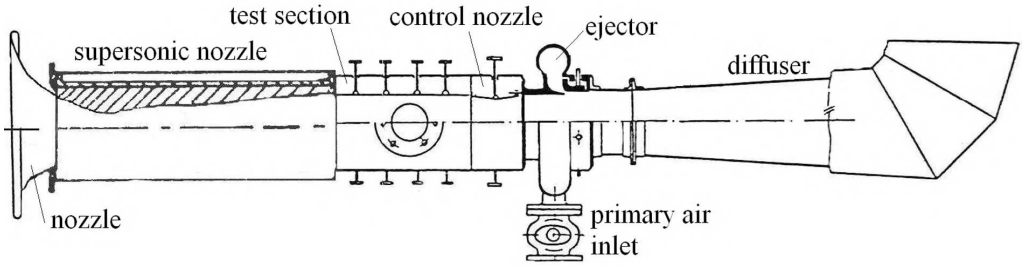

Fig. 1. Opened wind tunnel with ejector propulsion for $M > 1$

Most of the existing wind tunnels with the ejector propulsion use ejectors with a primary nozzle that is shaped as a slot. The slot is usually adjustable and it is used to control the primary mass flow rate as it was shown by Dvořák in [14]. The disadvantage of this arrangement is its lower efficiency in comparison with the circular nozzles ejectors as it follows from work [15] by Dvořák. There are several reasons for the low efficiency of this type of ejectors. Firstly, the primary nozzle has lower efficiency itself. Further, the higher velocity near the mixing chamber wall causes higher friction losses. For that reason, the construction of the ejector with several annular primary nozzles placed around the mixing chamber was designed by Kolář and Dvořák in work [16], which is shown in fig. 2. After the numerical calculations using this concept (presented by Kolář et. al in work [17]), it was found out that the efficiency is quite high, but it was necessary to solve the problem with the reversal flow in the mixing chamber. This reversal flow occurs in the center of the mixing chamber. The reversal flow is caused by an adverse gradient of the static pressure during the mixing processes, as Tesař showed in work [18].

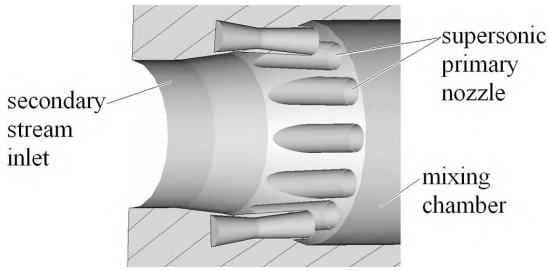

Fig. 2. The inlet part of the mixing chamber with annular supersonic nozzles around the mixing chamber wall [16]

2. Methods

2.1. Optimization method

The method presented in works [11] and [12] was used to optimize the supersonic ejector. This method was originally developed for optimization of axi-symmetric subsonic ejector. It is based on one-dimensional Gauss optimization method, where only one optimization parameter is changed in each optimization step. The optimization parameters are radial coordinates of selected control points on the wall of the ejector. The optimization method developed in work [11] has several disadvantages that follows from the fact that only one parameter is changed during each optimization step. Firstly, a large number of optimization steps (typically about 10^3) is necessary to obtain an optimal shape of the ejector. Further, a waviness of the ejector wall connected with local boundary layer separation can occur. It means that the movements of the control points are strongly non-uniform in these cases. If this happens the optimization fails and does not converge to the best solution. Both effects, the long optimization time and the wall waviness, are caused by controlled shifts of particular control points. The movement of control points, in which the objective function is not improved, is reduced. Later, the optimization in these points is interposed to accelerate the optimization of different parts of the ejector. Mentioned disadvantageous effects become serious during the optimization of a supersonic ejector. The occurrence of the wall waviness is followed by convergence problems. The complete optimization and numerical calculations themselves take immoderately long time. The time cost is higher also because of the three-dimensional geometry and high number of cells of the computational mesh.

The original optimization method [11] and its improvement are obvious from fig. 3. If the original method is used, the only one optimization parameter r_i is changed in each optimization

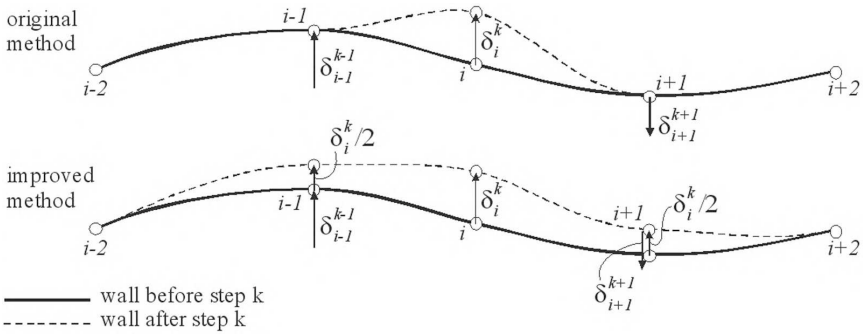

Fig. 3. Change of the ejector wall for original method (upper) and improved method (lower)

step k, i.e. only one control point i is moved by δ_i^k. Newly, except for the point i, points $i-1$ and $i+1$ are moved by $\delta_i^k/2$. Thus, the shift of the wall is more continual and influences longer part of the ejector. The number of backward steps, in cases of decrease of the objective function, is reduced. Situations, when the shifts of some points are extremely minimized, are practically eliminated. Faster optimization and prevention of the wall waviness are obtained as the result. For the resent work, 10 control points were use to optimize the shape of the ejector. The whole optimization runs automatically without any user interaction.

If an ejector is optimized, the objective function is the efficiency η defined by the relation

$$\eta = \frac{\dot{m}_2}{\dot{m}_1} \frac{\left(\frac{p_b}{p_{02}}\right)^{\frac{\kappa-1}{\kappa}} - 1}{1 - \left(\frac{p_b}{p_{01}}\right)^{\frac{\kappa-1}{\kappa}}} \frac{T_{01}}{T_{02}}, \tag{1}$$

where $\dot{m}_1$ and $\dot{m}_2$ are the mass flow rates of the primary and the secondary streams, p_{01} and p_{02} are stagnation pressures, T_{01} and T_{02} are stagnation temperatures, p_b is the back pressure and $\kappa = 1.4$ is the ratio of specific heats. Because all the boundary conditions are constant and also the mass flow rate of the primary stream changes only negligibly, the objective function is simplified to the mass flow rate $\dot{m}_2$ of the secondary stream.

2.2. Numerical model

Software Fluent 6.3.26 was used to calculate the flow in supersonic ejectors. The construction of the ejector and the boundary conditions are presented in fig. 4. Because of the ejector construction, the two-dimensional axi-symmetric calculation is not possible and the problem must be solved as a three-dimensional. The problem is solved as symmetrical along two planes that form an angle of $30°$. The total cross section area of the primary nozzles throats is 400 mm^2, with the outlet area ratio $A_{2exit}/A_{throat} = 2$ for design Mach number $M_1 = 2.2$. The length of the inlet part of the ejector is 120 mm. Initial diameter is 40 mm. The part containing the mixing chamber and the diffuser is 1 200 mm long with the initial diameter 68 mm. The pressure-based segregated solver was used, because provides very good convergence that is necessary for this optimization task. This solver uses a solution algorithm where the governing equations are solved sequentially (i.e., segregated from one another). Because the governing equations are non-linear and coupled, the solution loop must be carried out iteratively in order to obtain a converged numerical solution. With the segregated algorithm, each iteration consists of the steps outlined below: 1. Update fluid properties (e.g. density, viscosity, specific heat) including

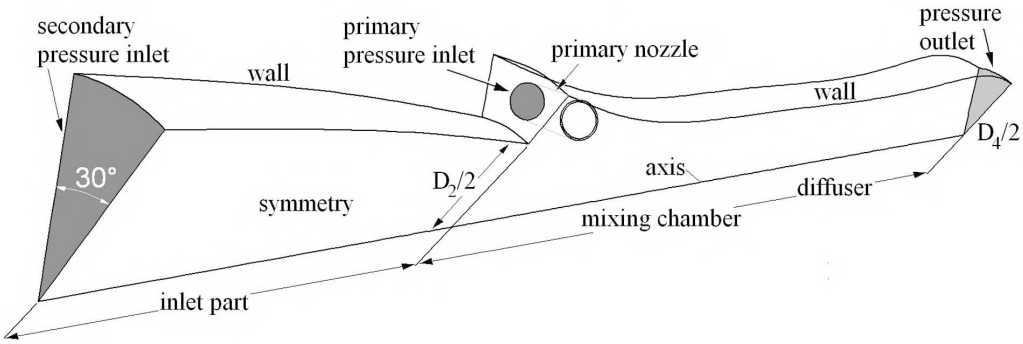

Fig. 4. Construction of the ejector and definition of boundary conditions

turbulent viscosity based on the current solution. 2. Solve the momentum equations, one after another, using the recently updated values of pressure and face mass fluxes. 3. Solve the pressure correction equation using the recently obtained velocity field and the mass-flux. 4. Correct face mass fluxes, pressure, and the velocity field using the pressure correction obtained from Step 3. 5. Solve the equations for additional scalars, if any, such as turbulent quantities, energy, species, and radiation intensity using the current values of the solution variables. These steps are continued until the convergence criteria are met, see documentation [19] for more details.

Stagnation pressure $p_{02} = 70$ kPa (absolute), stagnation temperature $T_{02} = 300$ K and turbulence intensity 30 % were used for inlet of the secondary air stream. The high turbulence intensity follows from consideration of flow behind the test section (e.g. behind a bluff body) of the wind tunnel. Stagnation pressure $p_{01} = 400$ kPa (absolute), stagnation temperature $T_{01} = 300$ K and turbulence intensity 10 % were used for inlet of the primary air stream. Back pressure $p_b = 100$ kPa (absolute) was used for outlet boundary condition. We used k-ω SST turbulence model that is suitable for calculation of flow in supersonic ejectors, as it was stated in work [20] by Kolář and Dvořák, in work [21] by Šimák or by Bartosiewicz et al. in work [22]. To compute the flow near the walls, the mesh was refined in such way that the wall adjacent cells had the width of 0.1 mm. As a result value $y^+ = 20 \div 30$ was obtained.

2.3. Dynamic mesh

A method of dynamic mesh provided by Fluent called "user defined deforming" was used. This method allows direct setup of positions of each node in the computational domain. The movements of the nodes are controlled by user defined functions. Fig. 4 shows completely deformed computational mesh of the model. In Cartesian coordinate system (x, y, z), the x values of all nodes are fixed during the optimization. Values of y and z are modified. In polar coordinate system (x, r, φ), values x and φ are fixed, while r is modified. Only the mesh inside and around the primary nozzle is an exception. The angle φ is transformed in such a way that the cross sections of the primary nozzle remain constant. Only the ejector axis is fixed, while the single cross sections of the primary nozzle are shifted in radial direction. The geometry of the primary nozzle is slightly deformed during its declination to the ejector axis. The final shape of the ejector wall is given by a natural cubic spline passing through the control points. The inlet part is described by different function than the part containing the mixing chamber. Deformation of the wall during the optimization is obvious from fig. 5.

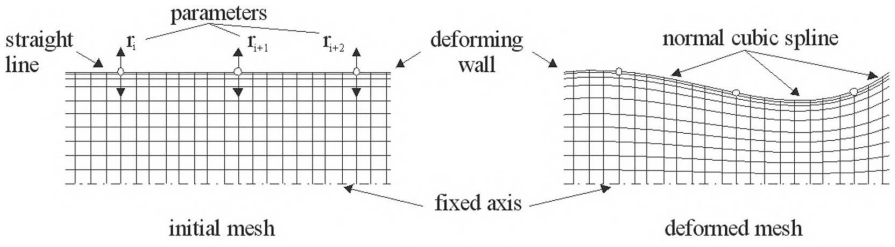

Fig. 5. Transformation of the wall during the optimization

3. Results

3.1. Final shapes of the ejector

The complete shapes of the ejector with the contours of Mach number are presented in fig. 6. Variant A is the initial shape of the ejector. It is interesting that even unoptimized ejector with

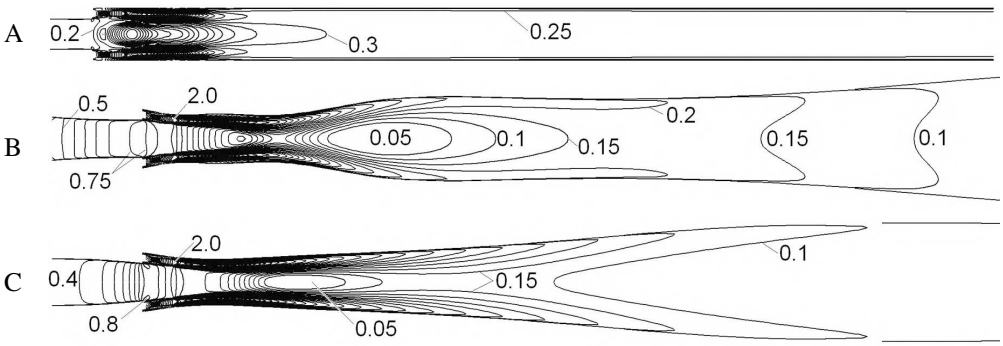

Fig. 6. Shapes of ejector with contours of Mach number, range $0 \div 2$; A – initial shape, B – optimized by original method, C – optimized by improved method

no declination of the primary nozzles and with no diffuser is able to operate with the positive secondary mass flow rate. We assume this to be caused by the fast mixing when twelve primary nozzles are used. Variant B is the ejector shape obtained by using the original optimization method after 763 steps. The optimization proceeded until the shifts of the control points became insignificant and the objective function stopped improving. Finally, variant C is the ejector obtained by use of the improved optimization method after 195 steps. Also here, the optimization was terminated after the objective function stopped to develop.

The wall waviness occurs for ejector B, as we can see in fig. 6 and in detail in fig. 7. Compared to ejector C with only one contraction, ejector B has three contractions. The flow field is thus decelerated and accelerated again. We can assume that this is not ordinary shape of the ejector. Nevertheless, the differences between the values of the objective function are negligible between both final shapes. Mass flow rates, efficiencies of the ejectors and geometry specification are contained in table 1.

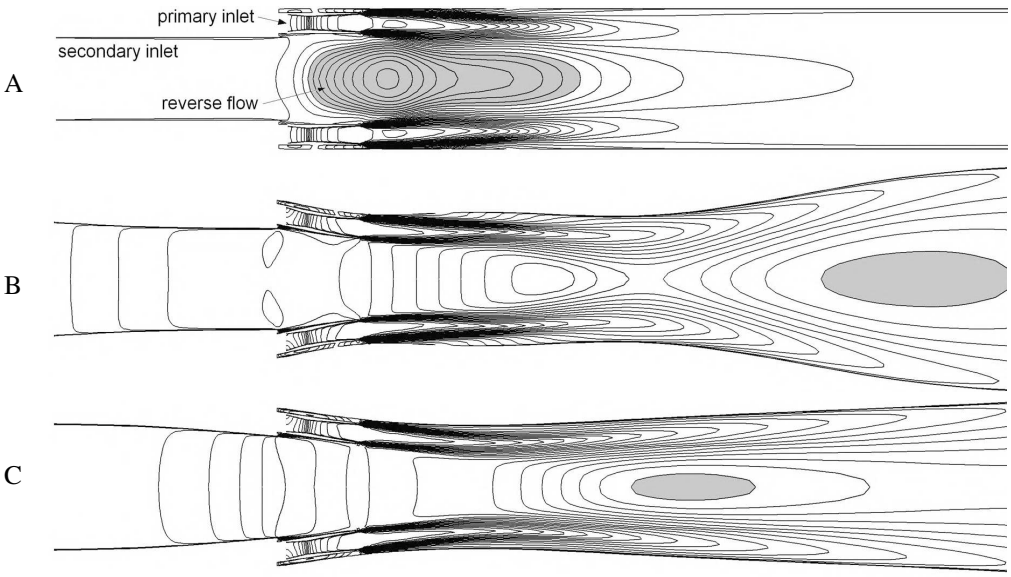

Fig. 7. Contours of x-velocity, range $-200 \div 500$ m/s. Areas of reversal flow are gray painted

Table 1. Mach numbers, mass flow rates, efficiencies and geometry specifications

	M_1 [–]	M_2 [–]	α [°]	D_2 [mm]	D_3 [mm]	D_4 [mm]	$\dot{m}_1$ [$\mathrm{kg \cdot s^{-1}}$]	$\dot{m}_2$ [$\mathrm{kg \cdot s^{-1}}$]	efficiency [%]
A	2.00	0.24	0	40	68	68	0.380 2	0.080 2	6.92
B	2.05	0.76	10.1	49.1	61.4	176.1	0.373 2	0.285 8	25.11
C	2.04	0.80	8.2	49.3	59.9	152.7	0.376 5	0.290 6	25.32

D_2 is diameter of the secondary air stream entry into the mixing chamber (see fig. 4), D_3 is the minimal diameter of the mixing chamber, D_4 is diameter of the outlet cross section of the ejector and α is declination of the primary nozzles. Ejector C is thinner than ejector B and primary nozzles have lower declination angle. This declination of primary nozzles causes elimination of the reversal flow.

Contours of axial velocity displayed on the plane of ejector axis and of the primary nozzle axis are presented in fig. 7. For all variants, areas of the reversal flow are painted in gray. For the initial ejector A, the area of reversal flow occupies the whole free space in the center of the mixing chamber. Reverse velocity reaches values of 200 m/s. Thus, the secondary air is sucked into the remaining space between primary nozzles. The mixing processes proceed only around the mixing chamber wall near the jets produced by the primary nozzles. A smaller area of reversal flow is also present in ejector B, but it is likely caused by faster expansion of the cross section of the ejector, than by low declination of the primary nozzles. The reverse velocity is only 25 m/s. The area of the reversal flow in ejector C is even smaller, but it is still present. It is caused by different declinations of primary nozzles, which are smaller for ejector C.

An analysis of flow in resulting ejector C is in fig. 8. There are contours of turbulent kinetic energy, Mach numbers and static pressure in the picture. Curves of static pressure and mass weighted turbulent kinetic energy throughout the mixing processes are carried out into the diagram. The initial region of mixing is marked in fig. 8. The initial region of mixing is characterised by the existence of the unaffected secondary stream, slow mixing and practically constant static pressure. The initial region ends in the narrowest cross section of the ejector – in the ejector throat. Here, the static pressure begins to rise rapidly, while the free shear layer (the mixing layer) does not reach the mixing chamber centre. In this case, the unaffected secondary stream still exists and vanishes later. Compared to the mixing with the only one primary nozzle placed in the axis of the ejector, the end of the mixing, i.e. the end of the main region of mixing and the beginning of the diffuser section can not be practically identified. Reversal flow in the centre of the mixing chamber is almost removed. As a result of the optimizaiton, the constant pressure initial mixing region was obtained, while the high efficiency of 25 % is caused by a rapid static pressure rise in the divergent mixing chamber.

3.2. Comparison of optimization methods

Courses of the objective function for both presented method of shape optimization of ejector are carried out in diagram on fig. 9. It is obvious from this picture that the improved method is definitely faster. For the original method, the development of the objective function becomes significantly slower after about 120 steps. The deceleration of improved method is evident after achievement of optimal shape. Reduction in the number of iteration steps is more than 50 % at the beginning of the optimization (first 50 steps). Later it can reach 80 %.

Another comparison of both methods is shown in diagram on fig. 10, where absolute values of shifts of the control points are recorded. The initial shifts of the control points are not

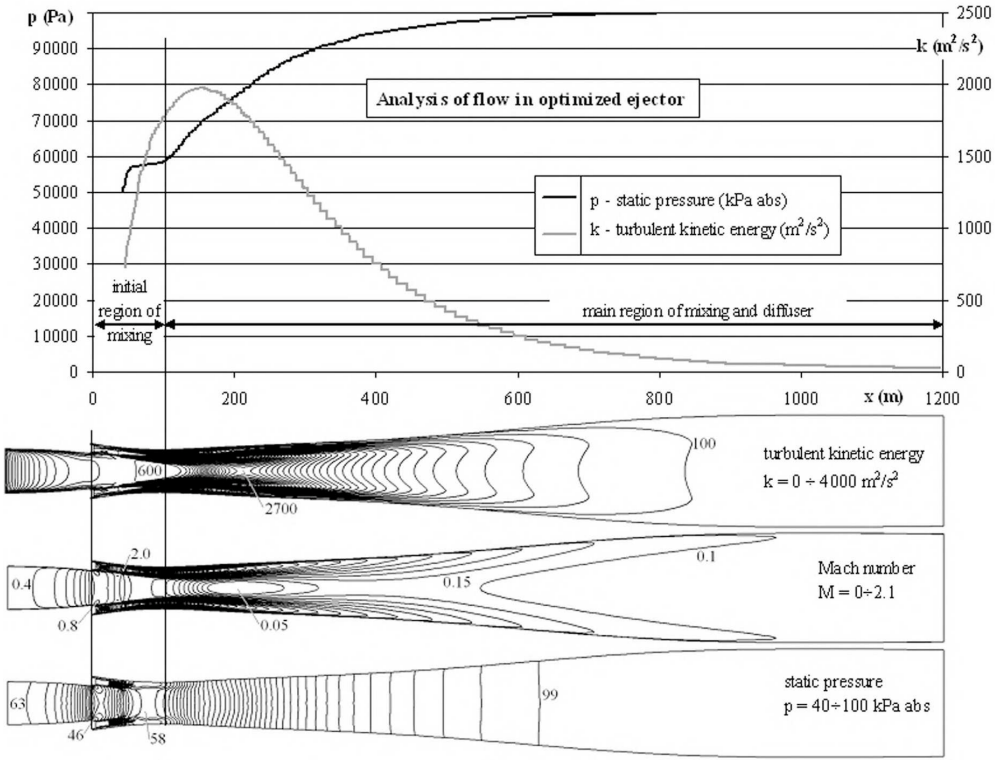

Fig. 8. Analysis of flow in the ejector C. Contours of turbulent kinetic energy, Mach numbers and static pressure. Curves of the static pressure and the mass weighted turbulent kinetic energy throughout the mixing process

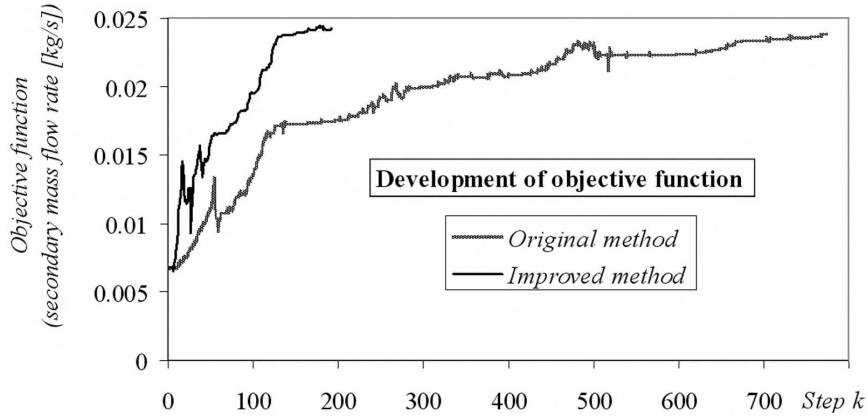

Fig. 9. Development of objective function for original and improved optimization methods

equal, but depend on the position of control points in the ejector. The shift of the point on the inlet of the secondary stream is smaller, than the shift at the end of the diffuser, where the faster widening of the cross section is expected. The smallest shift belongs to the point at the beginning of the mixing chamber. Single peaks in fig. 10, that repeat after 11 to 33 steps, represent shift of the last control point on the outlet of the ejector.

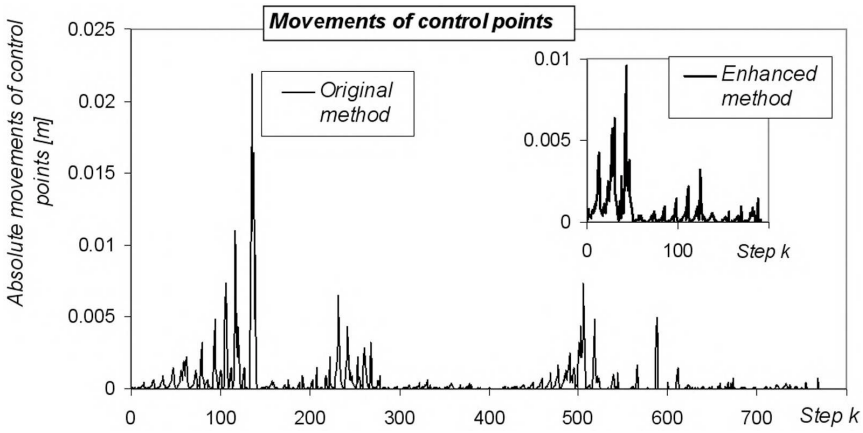

Fig. 10. Absolute values of shifts of control points during optimization for original and improved optimization methods

It can be observed from the curves in fig. 10 that the optimization runs in several periods for both methods. The correct direction of the optimization is found and the shifts are increased at the beginning of each period. The shifts become significant at the end of the period. In our case, the periods are terminated by a collapse of numerical solution. Then, the shifts are decreased and optimization continues.

4. Conclusion

An original method for the optimization of subsonic ejectors was improved to be also applied for supersonic ejectors. The improved method is definitely better. It is faster, steadier and more reliably to converge to the optimal solution. Nevertheless, the convergence problems of the numerical solution of the flow in the ejector were not completely removed. Thus, it would be helpful to adjust further the optimization method to avoid these problems.

Both methods were used to optimize the shape of a supersonic ejector for propulsion of an experimental wind tunnel. A construction of the ejector with twelve primary nozzles around the mixing chamber wall was optimized. As a result of the optimization, the primary nozzles are declined to the ejector axis. Thus, the reversal flow in the center of the mixing chamber is almost eliminated. As a result of the optimizaiton, the constant pressure initial mixing region was obtained, while the high efficiency of 25 % is caused by a rapid static pressure rise in the divergent mixing chamber. The optimization can be extended in the next work to optimize also the number of the primary nozzles.

Acknowledgements

This work was supported by the Czech Science Foundation, grant P101/10/1709 ”Nozzles and diffusers in ejectors”, and by the Research plan MSM 4674788501 funded by the Ministry of Education, Youth and Sports of the Czech Republic.

References

[1] Keenan, J. H., Neumann, E. P., Lustwerk, F., An Investigation of Ejector Design by Analysis and Experiment. Journal of Applied Mechanics, Trans ASME, 1950, 72, pp. A75–A81.

[2] Sun, D. W., Eames, I. W., Recent Developments in the Design Theories and Applications of Ejectors – a review. Journal of the Institute of Energy, 1995, pp. 65–79.

[3] Bonnington, S. T., King, A. L., Jet Pumps and Ejectors, a State of the Art; Review and bibliography (2nd edn). BHRA Fluid Eng, Cranfield, Bedford UK, 1976.

[4] Aphornratana, S., Eames, W. I., A Small Capacity Steam-ejector Refrigerator: Experimental Investigation of a System Using Ejector with Movable Primary Nozzle. International Journal of Refrigeration. Vol. 20, No. 5, 1997, pp. 352–358.

[5] Yadav, R. L., Patwardhan, A. W., Design Aspects of Ejectors: Effects of Suction Chamber Geometry. Chemical Engineering Science 63, 2008, pp. 3 886–3 897.

[6] Grazzini, G., Rocchetti, A., Numerical Optimisation of a Two-Stage Ejector Refrigeration Plant. International Journal of Refrigeration 25, 2002, pp. 621–633.

[7] Watanawanavet, S., Optimization of a High – Efficiency Jet Ejector by Computational Fluid Dynamics Software. Texas A&M University, May 2005.

[8] Cizungu, K., Groll, M., Ling, Z. G., Modelling and Optimization of Two-phase Ejectors for Cooling Systems. Applied Thermal Engineering 25, 2005, pp. 1 979–1 994.

[9] Riffat, B. S., Gan, G., Smith, S., Computational Fluid Dynamics Applied to Ejector Heat Pumps. Applied Thermal Engineering Vol. 16, No. 4, 1996, pp. 291–297.

[10] Rusly, E., Aye, Lu, Charters, W. W. S., A. Ooi: CFD Analysis of Ejector in a Combined Ejector Cooling System. International Journal of Refrigeration 28, 2005, pp. 1 092–1 101.

[11] Dvořák, V., Shape Optimization of Axisymmetric Ejector. Proceedings of European Conference on Computational Fluid Dynamics, Egmond aan Zee, 2006.

[12] Dvořák, V., Shape Optimization and Computational Analysis of Axisymmetric Ejector. Proceedings of the 8^{th} International Symposium on Experimental and Computational Aerothermodynamics of Internal Flows, Lyon, 2007, pp. 273–278.

[13] Dvořák, R., A contribution to the theory of ejection wind tunnel (Příspěvek k teorii ejekčního aerodynamického tunelu), Mechanical Journal (Strojnický časopis) XII, C. 1, 1. 6. 1961.

[14] Dvořák, R., Ejection wind tunnel ÚVS 180×250 mm^2 for high speeds (Ejekční aerodynamický tunnel ÚVS 180×250 mm^2 na vysoké rychlosti). Technical report č. 14/58, ČSAV, Ústav pro výzkum strojů. 1958.

[15] Dvořák, V., An ejector of classic construction combined with a slot nozzle. 4^{th} conference with international participation, Proceedings of Applied mechanics, Ostrava, Czech Republic, 2002, pp. 35–42.

[16] Kolář, J., Dvořák, V., Design of ejector for supersonic wind tunnel, Proceedings of the 26^{th} Meeting of Thermodynamic and Fluid Mechanic Department, Herbertov, Czech Republic, 2007, pp. 43–44.

[17] Kolář, J., Dvořák, V., Ščibran, P., Development of supersonic twelve driving nozzles ejector for supersonic wind tunnel. Proceedings of Experimental Fluid Mechanics, Liberec, 2007, Czech Republic, pp. 41–46.

[18] Tesař, V., Reversal paradox (Reverzační paradox). Acta Polytechnica – Práce ČVUT v Praze, 12 (II.2) 1984.

[19] Fluent 6.3 User's Guide, Fluent Inc. 2006.

[20] Kolář, J., Dvořák, V., Interaction of Shock Waves in Supersonic Ejector. Proceedings of the 27^{th} Meeting of Thermodynamic and Fluid Mechanic Departments, Plzeň, Czech Republic 2008.

[21] Šimák, J., Computation of the Flow and Interaction of Shock Waves in a 2D Supersonic Ejector, In: Colloquium Fluid Dynamics 2009, Institute of Thermomechanics AS CR, v.v.i., Prague, Czech Republic, October 21–23, 2009.

[22] Bartosiewicz, Y., Aidoun, Z., Desevaux, P., Mercadier, Y., Numerical and Experimental Investigations on Supersonic Ejectors. International Journal of Heat and Fluid Flow 26, 2005, p. 56–70.